Analysis of the rotational capability of the utilization of range of a spherical joint used in a passenger automobile McPherson suspension

Analysis of the rotational capability of the utilization of range of a spherical joint used in a passenger automobile McPherson suspension

S Para[1] and A Kuranowski[2]

[1,2] University of Technology, Cracow, PL

Email: aleksander.kuranowski@mech.pk.edu.pl, s.para@sbg.at

Abstract. In this paper a method is presented how to determine the utilization of range of rotational ability of a ball joint used in a passenger automobile McPherson suspension. A portable measurement arm was used to measure some vehicle's suspension geometry points as well as the geometry of suspension components. Based on the initial measured data a simulation model was used to estimate the real geometric parameters of the suspension and of the attachment points at the chassis. The damper module's top mount movement as well as the stiffness characteristics of the control arm bushing allow to simulate the utilization of range of motion capability of the spherical joint as result of the suspension movement under external loads. These loads can result from pass over a bump or cornering movements. The rotational ability of the ball joint and its applied loads can be input for further stiffness analyses by making use of FEM software.

1. Introduction

The considered suspension in this paper is a McPherson strut (see Figure 1) with the steering mechanism and steering rack. There are 6 moving components (control arm, wheel knuckle, steering rod, damper rod, wheel, steering rack), 2 cylindrical joints (A_1, B_0) and 4 spherical joint (B_1, B_3, A_2, A_3). It is a 5 DOF system with three local rotations: 1) of the steering rod, 2) the wheel, 3) the damper along its axes and two longitudinal motions: 4) movement of the damper during compression and rebound, 5) movement of the steering rack. All these movements regarded as one DOF separately. During the further procedure this suspension is analysed as a 2 DOF system (steering rack movement and damper length). The aim of this work is to determine the utilization of range of rotational capability of the spherical joint B_1. Its pivoting and rotational range primarily depend on the before described movements 4) and 5). The suspension is attached at points A_1 and A_2 through elastomer bushings and at a substitute point A_3 through a free of clearance ball joint to the chassis. Hence, the position of attachment points A_1 and A_2 change their position in the case of external forces. These forces occur during pass over a bump or during cornering.

In order to carry out this analysis numerically according to [2], real geometrical data was measured by making use of a mobile measuring arm by Faro (Gage Plus) [5]. The test object was a Ford Galaxy (Europe) with its year of manufacture in 1996 (1.9 dm^3 TDI, 66 kW). More information about the measurements at the vehicle and of some suspension components will be presented in the following chapters. Additionally, the approach of how the data was computed is shown. Results of this publication will be the estimated coordinates of the vehicle suspension and the rotational capability of the ball joint B_1, considering the deflections of the flexible bushings. This information can be used for

dimensioning this type of joints in McPherson suspensions. Furthermore, this data can be an input for stiffness analyses by making use of FEM software to calculate the stresses. It can be useful if the same joint will be reused in different vehicle models or after a face-lift, where the suspension or the mass may change.

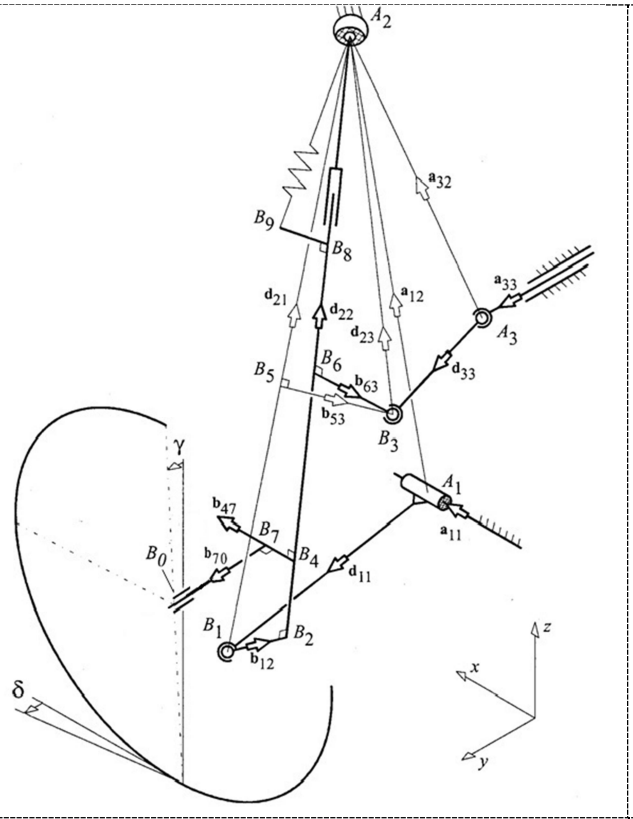

Figure 1. Schema of the front, left McPherson suspension including the steering mechanism.

δ – toe angle / γ – camber angle, both are defined positive into outside direction. (According to vehicle standards δ is defined positive into the inside direction)

A_1, A_2 movable connections of the suspension attached to the car body.

A_3 free of clearance connection to chassis.

B_1, B_3 free of clearance joints linked to suspension

B_0 wheel centre

a33 steering rack direction

d_{22} damper length

Coordinate origin lays in the longitudinal symmetry axis of the vehicle attached to the underbody (xy plane), global coordinate system

2. Data acquisition

In this chapter the approach to gain the needed data and finally the computed results are presented. The mobile measuring arm was used to measure the geometrical data at the vehicle and to measure suspension sub components. Additionally electronic scales were used to measure the horizontal load acting between wheel and ground. A MTS tensile test machine was used to gain the characteristics of the rocker arm bushing (A_1).

2.1. Measurement at the vehicle

To measure the toe and camber angle at different damper deflections and steering rack positions, the measuring arm Faro Gage Plus was used. Due to the relatively small measuring volume of 1200 mm (sphere) [5], the measurement had to be carried out in 2 measuring arm positions. First, the main coordinate system was defined. The xy plane was obtained by measuring four points (2 symmetrical) at the underbody. The x-axis is oriented into driving direction at the symmetry line. The y-axis lays at the xy-plane perpendicular to the x-axis. The z-axis results from the right hand rule. Within this global vehicle coordinate system, three measuring points (P_{1g}, P_{2g}, P_{3g}) were defined at different suspension components and their coordinates were stored. After that the measuring arm was moved to a place which was fixed to the car body and all measuring points at the suspension could be reached. Again the same defined points (P_{1m}, P_{2m}, P_{3m}) and all following points coordinates, according to the

measuring plan were collected. By carrying out the coordinate transformation from the moved coordinate system to the global coordinate system the numerical simulation could be carried out.

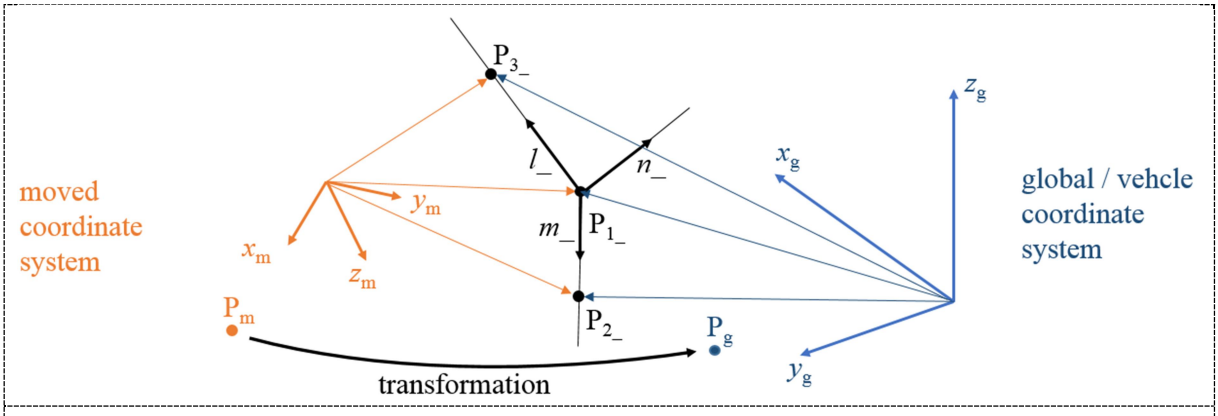

Figure 2. Coordinate transformation.

To transform the measured points from the moved coordinate system to the global / vehicle coordinate system two transformation matrices $\boldsymbol{M_m}$ (with P_{1m}, P_{2m}, P_{3m}) and $\boldsymbol{M_g}$ (with P_{1g}, P_{2g}, P_{3g}) had to be formed [3].

$$l_{\_} = |P_{3\_} - P_{1\_}| \qquad m_{\_} = \frac{(P_{2\_} - P_{1\_}) \times (P_{3\_} - P_{1\_})}{|(P_{2\_} - P_{1\_}) \times (P_{3\_} - P_{1\_})|} \qquad n_{\_} = l_{\_} \times m_{\_} \qquad (1)\ (2)\ (3)$$

$$\boldsymbol{M}_{\_} = \begin{bmatrix} l_{\_x} & l_{\_y} & l_{\_z} & 0 \\ m_{\_x} & m_{\_y} & m_{\_z} & 0 \\ n_{\_x} & n_{\_y} & n_{\_z} & 0 \\ P_{1\_x} & P_{1\_y} & P_{1\_z} & 1 \end{bmatrix} \qquad (4)$$

With the used vector operations (1) – (3) and matrices with (4) the transformation was calculated as follows:

$$P_g = P_m \cdot {M_m}^{-1} \cdot M_g \qquad (5)$$

The obtained global points were used to calculate the toe and camber angles as well as to estimate the parameters of the suspension. The comparison between measurement and simulation is presented in chapter 3.1.

2.2. Measurement of ball joint rotational capability

An angular rotation along the ball joint stub axis (1 in Figure 3) is 360 ° possible in any position. But the pivoting angle is limited due to its steel hull (2 in Figure 3). To measure the pivoting angle of the ball joint again the mobile measuring arm was used. Before the measurements were carried out, 3 cavities were drilled at the side of the screw nut, marked with orange areas in Figure 4 (one mark is at the reverse side). With these 3 measured points the centre of the screw was determined. The next step was to find the axis of the stub. Therefore 3 points were measured at the top side of the screw nut. A plane, which is perpendicular to the axis was obtained. Herewith the axes in 4 different maximum positions were gauged.

The measured pivoting angle τ between extreme positions I and II (see Figure 4) is 41.84°, whereas the measured angle between positions III and IV is 41.21°. To provide just one value for further analyses the arithmetic average of 41.5° is set.

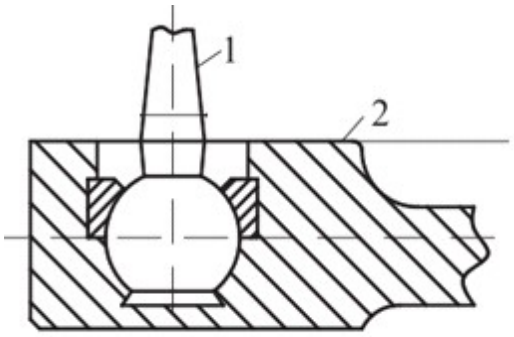

Figure 3. Ball joint scheme [1].

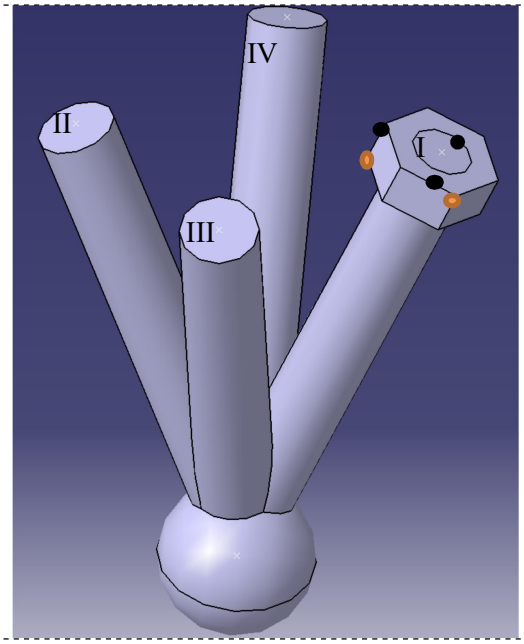

Figure 4. Measurement of stub axes.

2.3. Measurement of the upper bushing

The deflection of the upper bushing was captured with the measuring arm as well. Under different loads which acted vertically to the wheel the bushing moved as shown in the following figures. Red measuring points correspond do maximum right steering wheel turn. Green ones accord to straight ahead position and blue measuring points show the results of maximum left turn of the steering wheel. Here the explanation of the symbols: x (639 kg), • (500 kg), * (348 kg), ○ (148 kg), + (0kg). The green ring is the initial position with the straight ahead steering wheel at net weight of the car. The results show, that less vertical load to the wheel lets the bushing move outwards and downwards. A right turn causes the bushing move to the front of the car. In the other case the bushing moves backwards. Due to a difficult access to the bushing in the vehicle some measuring mistakes occurred at the blue cross or green star point. Nonetheless, a trend is recognizable. The maximum movement lays in a range of about 8 mm.

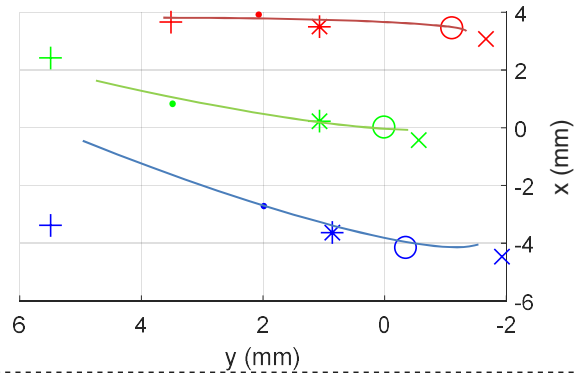

Figure 5. Bushing movement in xy plane.

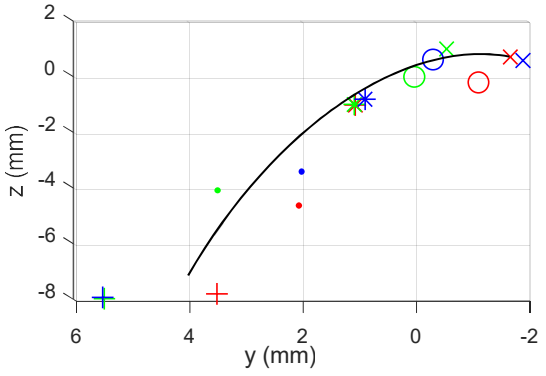

Figure 6. Bushing movement in yz plane.

2.4. Measurement of rocker arm bushing radial stiffness

The characteristics of the rocker arm bushing were measured at an MTS test rig. Two bushings of the same type but different manufacturer were compared. One was an old one (OEM), taken from the car junk yard. The elastomer was brittle and apparently with a high mileage. The second one was new. Below the result are presented.

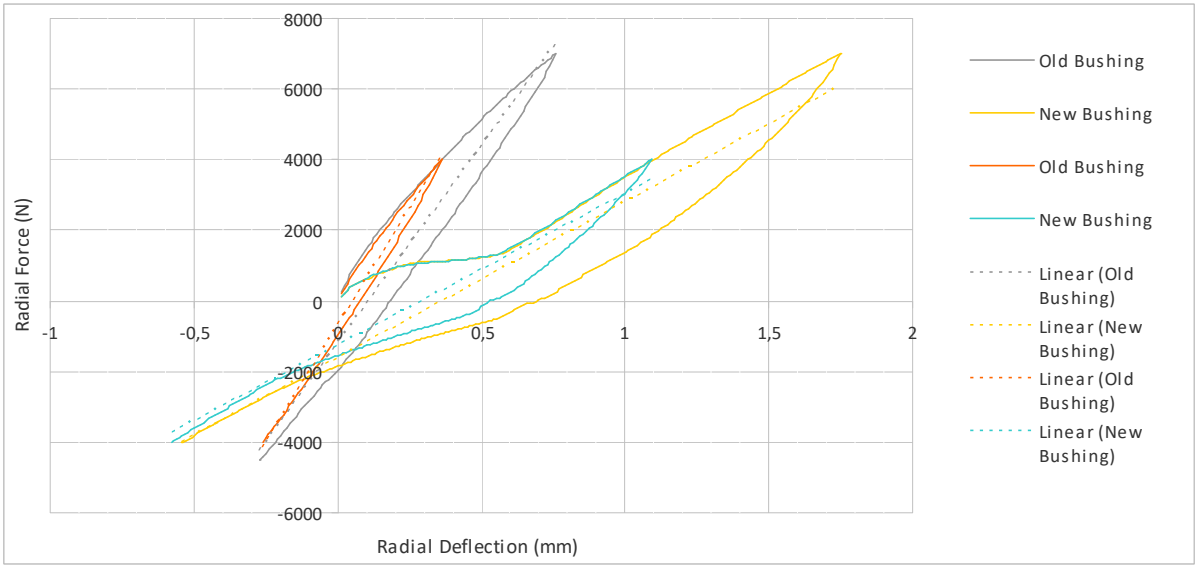

Figure 7. Measurement of rocker arm bushing force vs. deflection.

Measurements of two different bushings were carried out with two different positive/tensile maximum forces. One maximum cut-off force was 4000 N and the other was 7000 N. In negative/compression direction the maximum was set at 4000 N. Two different results can be noticed. The old bushing had a nearly 3 times higher stiffness, compared to the new one (~4.3 kN/mm). Real forces acting at the rocker arm in the vehicle are 4.0 kN and less. At this force a new bushing moves about 1 mm. Due to the fact that the bushing is symmetrical, it will be assumed that the deflection will occur in both directions.

3. Simulative modelling and results

This chapter will show the results of the carried out numerical analyses. The first step was to estimate the suspension parameters on the basis of the vehicle geometry measurements. With a working and correct suspension model the next step was to calculate the ball joint rotational capability. Inserting all knowledge of the suspension elements' deflection the capability was simulated.

3.1. Suspension parameter estimation

The following table show the coordinates of chassis connected suspension points (capital A letters) in the *global/vehicle coordinate system* and the estimated lengths in millimeter (lower case 'b' and 'd'). Where 'b' is the distance between points B (e.g. b12 between B1 and B2) and 'd' is the distance between points A and B (e.g. d11 between A1 and B1).

Table 1. Estimated suspension parameters

	A1	A2	A3	b12	b26	b63	d11	d33	b13
A_{ix}	315.8	242.4	142.6						
A_{iy}	391.1	552.5	373.3	89.5	36.7	146.2	348.6	314.5	193.3
A_{iz}	79.7	572.8	94.9						

Figure 8 shows the comparison between measured and simulated toe angle, based on the estimated values. Marked with an X the measured angles at the lowest position of the suspension (B_{0z} = -60 mm) and the nominal (normal) position of the vehicle (B_{0z} = 0 mm) are presented. The graph shows values in five different steering wheel positions which correspond to the steering rack movement: -95 mm (δ_{left} sim), -60 mm ($\delta_{left\ middle}$ sim), 0 mm (δ_{norm} sim), 60 mm ($\delta_{right\ middle}$ sim) and 95 mm (δ_{right} sim). The estimation accuracy lays in the range of less than 0.5°. The measurements were carried out at two suspension positions (damper lengths). By knowing, that the simulation procedure is valid [2], the angles in the maximum bump-in position (B_{0z} = 60) were computed.

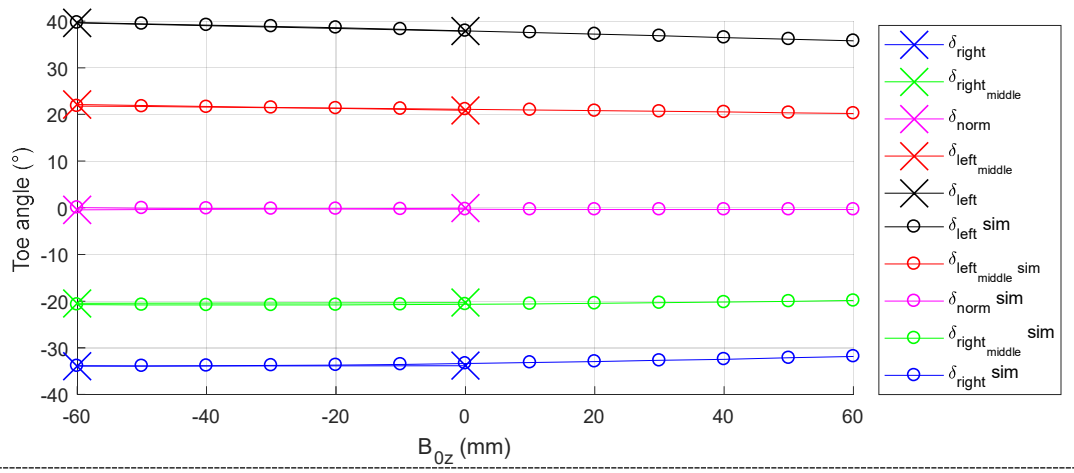

Figure 8. Toe angle as function of the vertical wheel knuckle movement B_{0z}. Measurement vs. simulation.

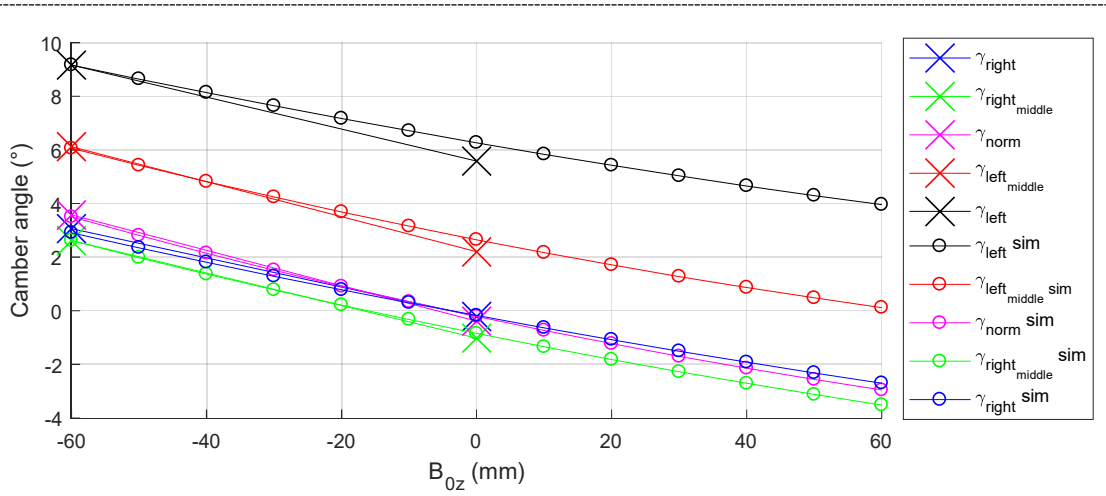

Figure 9. Camber angle as function of the vertical wheel knuckle movement B_{0z}. Measurement vs. simulation.

In Figure 9 the estimated results regarding the camber angle of the vehicle are presented. The line colours correspond to the same suspension and wheel positions as in Figure 8. The maximum error between measurement and simulation is less than 0.5°.

3.2. Simulative estimation of the utilized range of rotational capability of the ball joint

The rotational ability of the ball joint can be split up in two angles. The first is one corresponds to the toe angle (δ) of the wheel and lays in a range between -33.9° and 39.7°. The second is the pivoting angle (τ) which is dependent on the damper length or as shown in the following table on B_{0z}. Four scenarios were considered.

The first one shows the computed angles of a *rigid suspension*. All attachment points of the suspension to the car body do not move. The range of 26° lays between -16.3° and 9.7°.

In the second scenario only the *top mount deflection* was taken into account. This corresponds to a drive over a bump. Here, the range is 27.6°.

The third scenario, where only a *lower bushing deflection* occurs, can be explained by driving along a scarp. The main force acting on the wheel is in cross direction of the vehicle. The total calculated pivoting angle is 26°.

The last scenario is cornering which takes into account *both deflections*. Here, the car body rolls, which leads to damper deflection and an additional lateral force acts on the suspension. The maximum pivoting range is 27.6°.

Table 2. Pivoting angles **τ** of the ball joint (dependant on damper defection and toe angle)

		δ=-33.9°	δ=-20.0°	δ=0.0°	δ=21.1°	δ=39.7°
suspension rigid	B_{0z} = -60 mm	**1.1°**	**6.1°**	**9.0°**	**9.7°**	**9.0°**
	B_{0z} = +60 mm	**-16.3°**	**-11.8°**	**-8.8°**	**-8.1°**	**-8.6°**
top mount deflection	B_{0z} = -60 mm	**1.5°**	**6.9°**	**10.0°**	**10.5°**	**9.9°**
	B_{0z} = +60 mm	**-17.1°**	**-12.1°**	**-9.0°**	**-8.2°**	**-8.9°**
lower bushing deflection	B_{0z} = -60 mm	**0.8°**	**6.1°**	**9.1°**	**9.8°**	**9.1°**
	B_{0z} = +60 mm	**-16.2°**	**-11.7°**	**-8.8°**	**-8.1°**	**-8.7°**
both deflections	B_{0z} = -60 mm	**1.3°**	**6.9°**	**10.0°**	**10.6°**	**10.0°**
	B_{0z} = +60 mm	**-17.0°**	**-12.1°**	**-9.0°**	**-8.3°**	**-9.0°**

Comparing the measured pivoting angle of 41.5° to the maximum simulative angle of 27.6°, the utilized range within the vehicle suspension is 66%. This gives a possibility to reshape the ball joint hull and test the impact on the structure by making use of FEM software.

4. Conclusions and Outlook

In this paper an approach is presented, how to simulate the utilization of range of rotational capability of the ball joint in a vehicle McPherson suspension. Measurements were carried out with a mobile measurement arm. The measurement was influenced by the necessity of repositioning the arm. A coordinate transformation was carried out. Based on the measured points, the suspension parameters were estimated. Additionally the ball joint geometry and movement of the separated spare part were measured. With the used simulation procedure the utilization of range of rotary capability was calculated and compared to the measurements. The characteristics of the top mount and the lower rocker arm bushing were used within the simulation as additional information. The measured rotational capability of the ball joint lays in a range of 41.5°. Whereas the range used during the suspension movement, by taking into account deflections of the elastic elements, lays in a range of just 27.6°. This does mean, that 66% of the real joint pivoting capability is used. By knowing that fact, in a further step the steel hull can be adapted to analyse the load under reduced pivoting capability by making use of FEM software.

References

[1] Alexandru P, Visa I, Alexandru C 2014 Modeling the angular capability of the ball joints in a complex mechanism with two degrees of mobility *Applied Mathematical Modelling* **38** pp 5456-5470

[2] Knapczyk J, Para S 2012 Estimation of geometrical parameters of an elastokinematic model in a car McPherson suspension *Technical Transactions* **10**

[3] Meissonnier J, Fauroux J-C, Gogu G, Montezin C 2006 Geomietric identification of an elsatokinematic model in a car suspension *IMechE Vol. 220* Part D: J. Automobile Engineering pp 1209-1220

[4] Morecki A, Knapczyk J, Kędzior K 2002 Teoria mechanizmów i manipulatorów *Wydawnictwo Naukowo-Techniczne Warszawa*

[5] Niemczyk G 2005 Wpływ właściwości przegubów na charakterystyki siłowe układu kierowniczego samochodu *Doktoral Thesis Politechnika Krakowska*

[6] http://www.dirdim.com/pdfs/DDI_FARO_Gage.pdf 2018